Received: 5 May 2023 | Revised: 9 October 2023 | Accepted: 11 October 2023

DOI: 10.1111/mmi.15185

RESEARCH ARTICLE

WILEY

Lipidome remodeling in response to nutrient replenishment requires the tRNA modifier Deg1/Pus3 in yeast

Gabriel Soares Matos[1] | Leonie Vogt[2] | Rosangela Silva Santos[3] | Aurélien Devillars[2] | Marcos Yukio Yoshinaga[3] | Sayuri Miyamoto[3] | Raffael Schaffrath[2] | Monica Montero-Lomeli[1] | Roland Klassen[2]

[1]Instituto de Bioquímica Médica Leopoldo de Meis, Universidade Federal do Rio de Janeiro, Rio de Janeiro, Brazil

[2]Institut für Biologie, Fachgebiet Mikrobiologie, Universität Kassel, Kassel, Germany

[3]Department of Biochemistry, Institute of Chemistry, University of São Paulo, São Paulo, Brazil

Correspondence
Monica Montero-Lomeli, Instituto de Bioquímica Médica Leopoldo de Meis, Universidade Federal do Rio de Janeiro, Rio de Janeiro, Brazil.
Email: montero@bioqmed.ufrj.br

Roland Klassen, Institut für Biologie, Fachgebiet Mikrobiologie, Universität Kassel, Kassel 34132, Germany.
Email: roland.klassen@uni-kassel.de

Funding information
Conselho Nacional de Desenvolvimento Científico e Tecnológico; Deutsche Forschungsgemeinschaft, Grant/Award Number: KL2937/1, SCHA750/18, SCHA750/19 and SCHA750/20; Fundação Carlos Chagas Filho de Amparo à Pesquisa do Estado do Rio de Janeiro, Grant/Award Number: E26/201.070/2021 and E26/210446/2019; Fundação de Amparo à Pesquisa do Estado de São Paulo, Grant/Award Number: CEPID-Redoxoma 13/07937-8 and CNPq 313926/2021-2

Abstract

In the yeast *Saccharomyces cerevisiae*, the absence of the pseudouridine synthase Pus3/Deg1, which modifies tRNA positions 38 and 39, results in increased lipid droplet (LD) content and translational defects. In addition, starvation-like transcriptome alterations and induced protein aggregation were observed. In this study, we show that the *deg1* mutant increases specific misreading errors. This could lead to altered expression of the main regulators of neutral lipid synthesis which are the acetyl-CoA carboxylase (Acc1), an enzyme that catalyzes a key step in fatty acid synthesis, and its regulator, the Snf1/AMPK kinase. We demonstrate that upregulation of the neutral lipid content of LD in the *deg1* mutant is achieved by a mechanism operating in parallel to the known Snf1/AMPK kinase-dependent phosphoregulation of Acc1. While in wild-type cells removal of the regulatory phosphorylation site (Ser-1157) in Acc1 results in strong upregulation of triacylglycerol (TG), but not steryl esters (SE), the *deg1* mutation more specifically upregulates SE levels. In order to elucidate if other lipid species are affected, we compared the lipidomes of wild type and *deg1* mutants, revealing multiple altered lipid species. In particular, in the exponential phase of growth, the *deg1* mutant shows a reduction in the pool of phospholipids, indicating a compromised capacity to mobilize acyl-CoA from storage lipids. We conclude that Deg1 plays a key role in the coordination of lipid storage and mobilization, which in turn influences lipid homeostasis. The lipidomic effects in the *deg1* mutant may be indirect outcomes of the activation of various stress responses resulting from protein aggregation.

KEYWORDS
lipid droplets, lipidome, pseudouridine, storage lipids, tRNA, yeast

Gabriel Soares Matos and Leonie Vogt contributed equally.

1 | INTRODUCTION

Transfer RNA undergoes extensive post-transcriptional modification, which is important for structural integrity and functional efficiency in translation (Phizicky & Hopper, 2010). Deg1 is a tRNA pseudouridine synthase specifically modifying tRNA positions 38 and 39 (Lecointe et al., 1998). Absence of functional Deg1 causes pleiotropic phenotypes including slow growth and temperature sensitivity in yeast, and mutation of the human orthologue Pus3 is linked to neurodevelopmental disorders (Abdelrahman et al., 2018; Han et al., 2015; Lecointe et al., 1998; Lin et al., 2022; Shaheen et al., 2015, 2016). For yeast, pseudouridylation of tRNA-^{Gln}UUG by Deg1 is critical to maintain full decoding efficiency, but does not affect the cellular levels of this tRNA (Han et al., 2015; Klassen et al., 2016). Absence of Deg1 led to specific loss of U38 and U39 pseudouridylation, without effects on secondary modifications that were detected in other modification mutants (Barraud et al., 2019; Han et al., 2015; Tavares et al., 2021). Consistent with a reduced function of tRNA^{Gln}UUG in decoding, loss of Deg1 impairs protein biosynthesis of Gln-rich proteins such as the Rnq1 prion (Klassen et al., 2016). Similar to Elongator mutants, which lack critical modifications of wobble uridines, such as 5-methoxycarbonylmethyl(-2-thio)uridine [mcm^5(s^2)U] (Schaffrath & Leidel, 2017), *deg1* mutants display phenotypes indicative of nutrient signaling defects (Chou et al., 2017; Han et al., 2018; Klassen & Schaffrath, 2017). For example, Elongator and *deg1* mutants commonly upregulate the amino acid gene transcription factor *GCN4* and affect cellular amino acid levels (Chou et al., 2017; Mülleder et al., 2016). In addition, both mutants are sensitive to the Target of Rapamycin Complex 1 (TORC1) inhibitor drug rapamycin and combined *elp3 deg1* mutants trigger gene expression changes and autophagy activation consistent with reduced TORC1 activity (Bruch et al., 2020; Khonsari et al., 2021; Klassen & Schaffrath, 2017). A further similarity between *deg1* mutants and mcm^5(s^2)U defective cells is the induction of protein aggregates (Khonsari et al., 2021; Nedialkova & Leidel, 2015; Tavares et al., 2021), which may be caused by a ribosomal slowdown at specific codons during translation (Chou et al., 2017), increased frequencies of translational errors or both.

In a previous study, we have shown that absence of either Elongator or Deg1 function causes an imbalance in neutral lipid levels (Bozaquel-Morais et al., 2018). Both deletion strains present a higher content of lipid droplets (LD), which store the neutral lipids triacylglycerol (TG) and steryl ester (SE), and are more resistant to the acetyl-CoA carboxylase (Acc1) inhibitor soraphen A (sorA). Acc1 is the main regulator of fatty acid synthesis and catalyzes carboxylation of acetyl-CoA to malonyl-CoA, the building block of lipids. It is finely regulated by the AMPK/Snf1 kinase, which upon phosphorylation, inhibits Acc1 activity (Figure 1a). Deletion of AMPK/Snf1 in yeast leads to a high LD phenotype, inability to ferment sucrose and to inositol auxotrophy (Bozaquel-Morais et al., 2010, 2017; Shirra et al., 2001). The first trait is attributed directly to Acc1 hyperactivity. Another report that studied hyperactivity of Acc1 by substituting the phosphorylatable serine residue (S1157A) has shown that Acc1 phosphorylation regulates the proportion of C16 and C18 fatty acids in free fatty acids, glycerophospholipids and neutral lipids (Hofbauer et al., 2014). This regulation controls the proper functioning of membranes through sequestration of the transcription factor Opi1 by binding to C16 phosphatidic acids, leading to AMPK/Snf1 regulation of fatty acid chain length. As phosphatidic acid is an intermediate between TG and phospholipid synthesis, their synthesis is coordinated. It was also reported that Acc1 overexpression regulates the sterol and squalene content of the cell (Shin et al., 2012) showing tight coupling between Acc1 activity, neutral lipid and phospholipid synthesis to ensure lipid homeostasis. In this study, we investigated the lipid-specific effects of *deg1* mutation in more detail. Our results show that a *deg1* mutant deregulates the coupling between neutral lipid synthesis and phospholipids, leading to an imbalance between TG, SE and phospholipids during growth, independently of Acc1 activity.

2 | RESULTS

2.1 | Genetic interaction of *deg1* and *ACC1*^{S1157A} in soraphen A resistance

It was previously shown that a *deg1* mutation induces partial resistance against the Acc1 inhibitor sorA and increases cellular LD content (Bozaquel-Morais et al., 2018). In some cases, loss of tRNA modifications is known to cause tRNA destabilization via the activation of exonucleolytic decay, which is routinely suppressed by mutation of *MET22* (Phizicky & Hopper, 2023; Figure S1a). Since *MET22* is neither required for the high LD nor the sorA resistance phenotypes of *deg1* (Figure S1b,c), tRNA destabilization is unlikely mechanistically involved. Consistent with this assumption, a previous study revealed in *deg1* mutants unaltered levels of tRNA^{Gln}UUG, a tRNA that critically depends on the Deg1-dependent pseudouridylation for function (Han et al., 2015). Since upregulation of Acc1 activity affects LD and sorA phenotypes in a similar manner (Hofbauer et al., 2014), we investigated whether the *deg1* effect might occur through Acc1 activation, possibly due to interference with the inhibitory phosphorylation at S1157 (Figure 1a). We generated a yeast mutant carrying the hyperactivated *ACC1*^{S1157A} allele, that has been shown to be resistant to sorA (Hofbauer et al., 2014; Shen et al., 2004; Vahlensieck et al., 1994), as the only source of Acc1 and deleted the *DEG1* gene in this background. When the sorA phenotypes of the respective single mutants and the double mutants were compared, additive resistance was observed (Figure 1b). Hence, *deg1* mutation can increase sorA resistance in a background where inhibitory phosphorylation of Acc1 at S1157 is prevented. To test whether other potential Snf1-dependent phosphorylation sites (such as S659; Shi et al., 2014) are involved in the sorA phenotype of *deg1* cells, we combined *deg1* and *snf1* mutations and compared single and double mutant sorA phenotypes. Additivity in sorA resistance was again observed (Figure 1d), indicating that the *deg1* effect on sorA resistance (and potentially Acc1 activity) hardly arises from

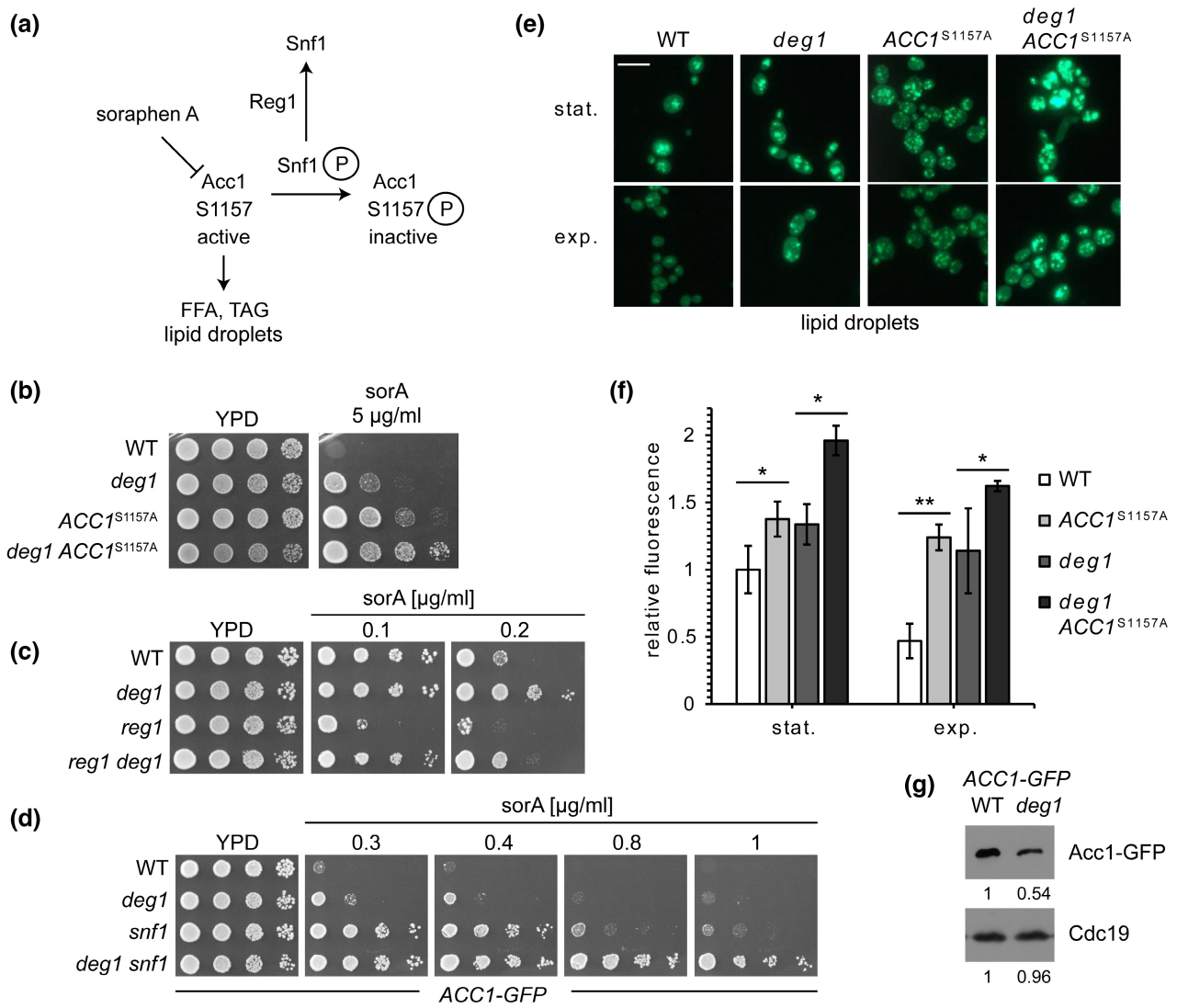

FIGURE 1 Additivity of lipid-related phenotypes of *ACC1*^{S1157A} and *deg1* mutants. (a) Scheme depicting the roles of Snf1, Reg1 and soraphen A (sorA) in the regulation of Acc1 activity. See text for details and references. (b) SorA phenotype of wild type (WT), *deg1*, *ACC1*^{S1157A} and the respective double mutant. (c) SorA phenotype of WT, *deg1*, *reg1* and the respective double mutant. (d) SorA phenotype of WT, *deg1*, *snf1* and the respective double mutant. Note that all strains used in this assay contain the *ACC1*-GFP fusion as the only source of Acc1, which increases sorA sensitivity. (e) Representative fluorescence-microscopic visualization of BODIPY493/503 stained yeast cells with the indicated genotypes. Staining was done with stationary phase cells (stat.) and after refeeding of cells with fresh medium, followed by 6 h growth into exponential phase (exp.). Scale bar = 10 µm. (f) Relative fluorescence of strains shown in (g). Cells were fixed, stained with BODIPY493/503 and examined at magnification 400×. Fluorescence was measured using ImageJ and normalized to wild-type stationary phase levels. The significance was determined utilizing two-tailed *t*-test (*≤0.05; **≤0.01). (g) Western blot analysis of Acc1-GFP and Cdc19 protein levels of WT and *deg1* cells. Signal intensities for the *deg1* strain were normalized to WT and are indicated.

changes in Snf1-dependent Acc1 phosphorylation targets. To verify that the S1157 phosphoregulation circuit in *deg1* mutants is in general functional, we removed the negative Snf1 regulator Reg1 (Ruiz et al., 2011; Figure 1a) and tested for alteration of the *deg1* sorA phenotype. Yeast mutants lacking *REG1* were previously shown to exhibit a lowered LD level and increased sorA sensitivity (Bozaquel-Morais et al., 2010). As expected for a situation where Snf1 can still be activated and inhibit Acc1 via phosphorylation, increased sorA sensitivity was observed in absence of Reg1 regardless of the presence or absence of Deg1. Therefore, phosphoregulation of Acc1 via Snf1 is functional in the *deg1* mutant (Figure 1c).

2.2 | Quantification of specific decoding errors in *deg1* mutants

To obtain a more comprehensive picture of the effect of *deg1* mutation on overall decoding, we mined a previously published transcriptional profiling data set for various tRNA modification mutants (Chou et al., 2017) and extracted ribosomal A-site occupancy changes for all codons in *deg1* mutants normalized to the wild type. As shown in Figure S2a, several codons display higher A-site occupancy in *deg1* mutants, including the Gln CAA codon as well as the Asn codons AAC and AAU. Higher A-site occupancy implies

that the ribosome slows down at these codons during translation and indicates a reduced decoding efficiency in the *deg1* mutant. Similar to the CAA decoder $tRNA^{Gln}UUG$, $tRNA^{Asn}GUU$, decoding both AAC and AAU also contains a Deg1-mediated pseudouridine (Boccaletto et al., 2018; Jühling et al., 2009). We focused on these three codons for further analysis, since in vivo misreading reporters were available (Salas-Marco & Bedwell, 2005) and allowed the quantification of translational errors that might be associated with ribosomal slow-down in *deg1* mutants. The assay utilizes a dual luciferase reporter encoding a renilla-firefly luciferase (R-luc/F-luc) fusion protein. In addition to a control encoding functional R-luc/F-luc, plasmids were used that encode mutated F-luc variants (K529N, K529Q and H245Q), which are inactive but can regain activity due to specific decoding errors (Figure S2b). In detail, misreading of Asn codons AAC or AAU by $tRNA^{Lys}$ in absence of Deg1-dependent modification of $tRNA^{Asn}$ may be increased and cause restoration of active $F\text{-}luc^{K529N}$. An analogous misreading event triggered by inefficient decoding by a hypomodified tRNA was previously demonstrated (Khonsari & Klassen, 2020). Similarly, misreading of CAA by $tRNA^{His}$ in $F\text{-}luc^{H245Q}$ or by $tRNA^{Lys}$ in $F\text{-}luc^{K529Q}$ may be promoted by inefficient decoding of the CAA codon in *deg1* mutants. Neither $tRNA^{Lys}UUU$ nor $tRNA^{His}GUG$, which could misread AAC/AAU or CAA, respectively and subsequently restore F-luc activity, contain a Deg1-dependent pseudouridine (Boccaletto et al., 2018; Jühling et al., 2009). We measured F-luc/R-luc ratios of the different reporters and the control encoding fully active luciferases from 10 biological replicates for each construct/mutant and calculated misreading frequencies by normalizing F-luc/R-luc ratios for the mutant plasmids (pDB825, pDB827, pDB872 and pDB865) to the control encoding fully active luciferases (pDB688; Figure S2). Indeed, *deg1* mutants displayed increased error rates at AAC and AAU codons, whereas no significant change was recorded for the two CAA misreading reporters. It should be noted that other misreading events at the CAA codon (e.g., by a distinct tRNA, which cannot be assessed with this assay) may still be increased. Results obtained for AAC/AAU misreading, however, demonstrate that specific misreading events are indeed elevated in *deg1*.

2.3 | Effect of *deg1* mutation on LD levels in absence of inhibitory Acc1 phosphorylation

Since the genetic interaction of *deg1* and $ACC1^{S1157A}$ in sorA resistance argued for an S1157-phosporylation independent effect in the tRNA modification mutant, we compared cellular LD levels in WT, *deg1*, $ACC1^{S1157A}$ and the double mutant in both, stationary and exponential growth phases. As previously described (Bozaquel-Morais et al., 2018; Hofbauer et al., 2014), both single mutations led to an increase in total LD levels as detected by BODIPY staining (Figure 1e). Importantly, we observe a further increase in LD levels in the double mutant (*deg1* $ACC1^{S1157A}$) when compared to either single mutant (Figure 1e,f). This result suggests that the tRNA modification defect can increase LD levels via a mechanism that is not entirely dependent on changes in the phosphorylation status of S1157 in Acc1.

Since Deg1 is important for decoding of several codons (Figure S2a) and improves functioning of tRNA in translation (Han et al., 2015; Klassen et al., 2016), we reasoned that its absence may affect the biosynthesis and cellular availability of Acc1. To test this, we utilized a strain expressing Acc1-GFP (enabling detection of Acc1 levels), introduced a *deg1* deletion and compared Acc1-GFP protein levels by Western analysis. As shown in Figure 1g, the tRNA modification mutant indeed exhibits reduced Acc1-GFP levels, despite the increased tolerance toward the Acc1 inhibitor drug. Thus, a translational defect of Acc1 mRNA or decreased protein stability might account for reduced Acc1 levels and the observed sorA and LD phenotypes are not linked to increased Acc1 levels in absence of Deg1.

2.4 | Genetic interaction of *deg1* and $ACC1^{S1157A}$ with respect to growth in absence of inositol

Transcription of *INO1* encoding inositol-3-phosphate synthase (Donahue & Henry, 1981) is known to be regulated by Acc1 activity. In the presence of activated Acc1, *INO1* expression is downregulated resulting in reduced growth on inositol-free medium (Hofbauer et al., 2014). Hence, if *deg1* mutation would upregulate Acc1 activity by interference of S1157 phosphorylation or through a different mechanism, reduced growth on inositol-free medium would be expected. Investigation of this phenotype, however, revealed that *deg1*, unlike $ACC1^{S1157A}$, does not reduce growth in absence of inositol. Instead, loss of *DEG1* partially rescues inositol-free growth of the $ACC1^{S1157A}$ mutant, suggesting an Acc1-independent effect on lipid homeostasis (Figure 2a). Similar to *deg1* mutation, loss of the transcriptional repressor Opi1 was also shown to suppress the inositol auxotrophy of an $ACC1^{S1157A}$ mutant by restoring *INO1* expression (Hofbauer et al., 2014). Loss of Opi1 was also reported to result in inositol overproduction and secretion (Greenberg et al., 1982). Since *deg1* equals *opi1* in genetic interaction with $ACC1^{S1157A}$ on inositol-free medium, we tested whether *deg1* mutation also induces inositol secretion. While inositol secretion of *opi1* mutants was verified, no such effect is presented by the *deg1* mutant (Figure 2b).

2.5 | Quantification of triacylglycerol and SE levels by thin layer chromatography

Since genetic analysis presented above suggested differential effects of $ACC1^{S1157A}$ and *deg1* on lipid-related phenotypes, we directly compared neutral lipid levels in WT, *deg1* and $ACC1^{S1157A}$ mutants in both exponential and stationary growth phases by thin layer chromatography (TLC) (Figure 3a). As shown by densitometric analysis of TLC images (Figure 3b), $ACC1^{S1157A}$ mutation resulted in

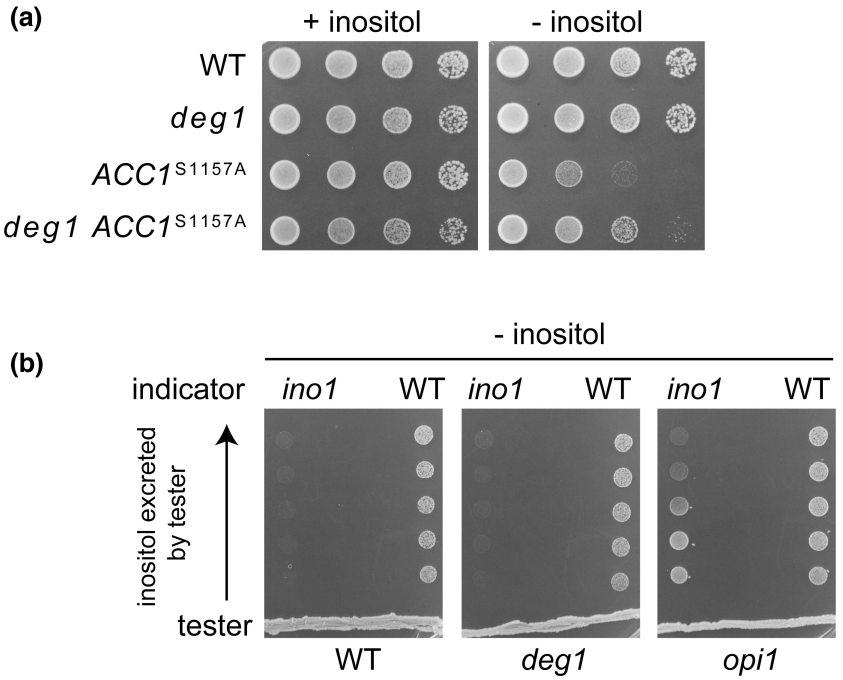

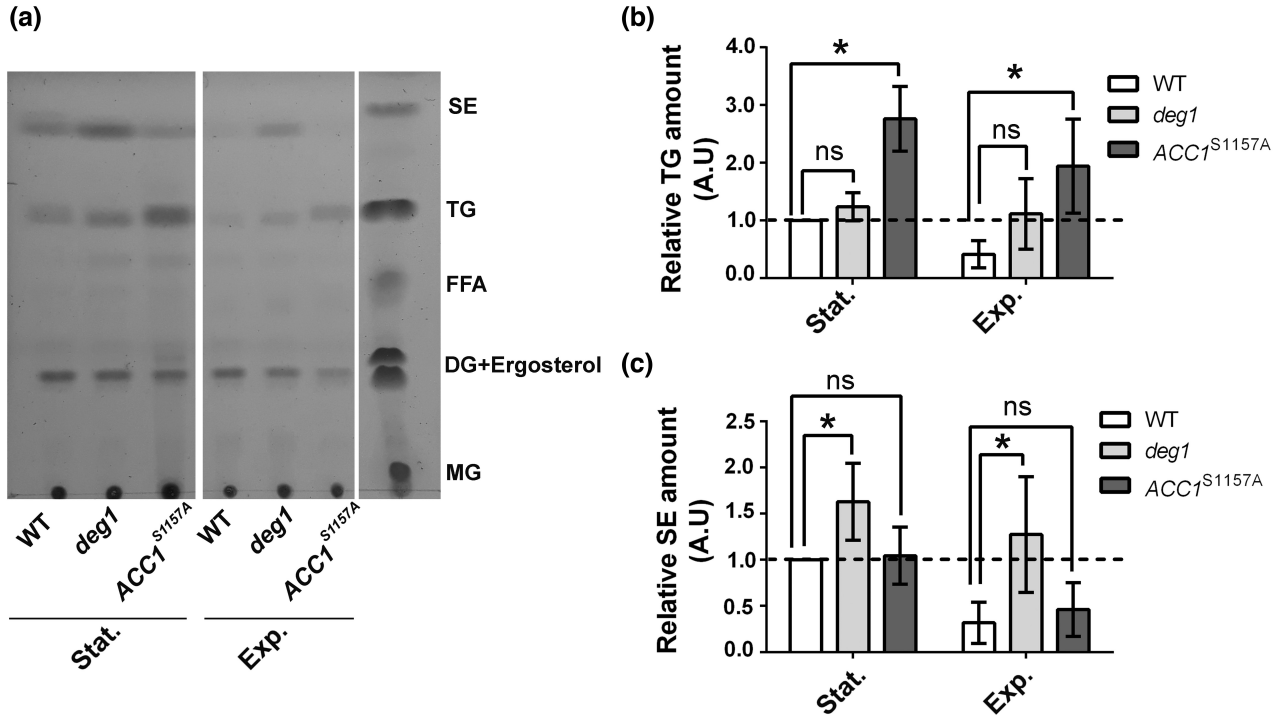

FIGURE 2 Inositol phenotypes of *ACC1*^{S1157A} and *deg1* mutants. (a) Growth of the indicated strains was determined in YNB-based minimal medium containing (+) or lacking (−) inositol. (b) Inositol excretion assay for WT, *deg1* and *opi1* (control) cells. Strains were streaked at the bottom of a YNB plate lacking inositol. At a 90° angle, 5 spots of cell suspensions (5 μL, OD600 nm = 1) of the indicator/control strains *ino1* and WT were applied. The *ino1* indicator strain can only grow if the tester strain excretes inositol into the medium. The *opi1* strain is known to excrete inositol and was employed as a positive control.

FIGURE 3 SE and TG levels in WT, *deg1* and Acc1^{S1157A} strains. (a) TLC and (b) Densitometric TLC analysis of steryl ester (SE) and triacylglycerol (TG) from WT, *deg1* and *ACC1*^{S1157A} strains grown to stationary (Stat) and exponential (Exp) phase. Data are shown as mean ($n = 3$) ± standard deviation of mean (SD). The significance was determined utilizing two-tailed *t*-test (*≤0.05; ns, non-significant).

a drastic increase in TG levels in both growth phases, which is in agreement with previously published data (Hofbauer et al., 2014). In contrast, loss of Deg1 hardly affected TG levels in the stationary phase and led to a moderate increase in the exponential phase of growth. Instead, SE levels were heavily induced in *deg1*, but not in *ACC1*^{S1157A} and this effect was detected in both, exponential and stationary phase. Thus, *deg1* mutation significantly impacts neutral lipid composition with a strong upregulation of SE and more moderate induction of TG. We assume that the effect of increased LD abundance in the tRNA modification mutant involves an alteration of the relative abundances of the two neutral lipids present in this organelle.

2.6 | Global effect of *deg1* mutation on the lipidome

Since the investigation of neutral lipid contents in *deg1* mutant revealed a major shift in SE abundance, we considered the possibility that additional lipid classes are affected by the loss of the Deg1-dependent tRNA modification. Assessment of 207 lipid species by UPLC-ESI-TOF/MS in the WT and the *deg1* mutant in stationary and exponential growth phases indeed revealed significant alterations in the cellular levels of 105 species (Table S1). These altered lipid species are represented by glycerophospholipids, SE, cardiolipin, and particularly multiple TG species. Heatmap analysis (Figure 4a,b) using

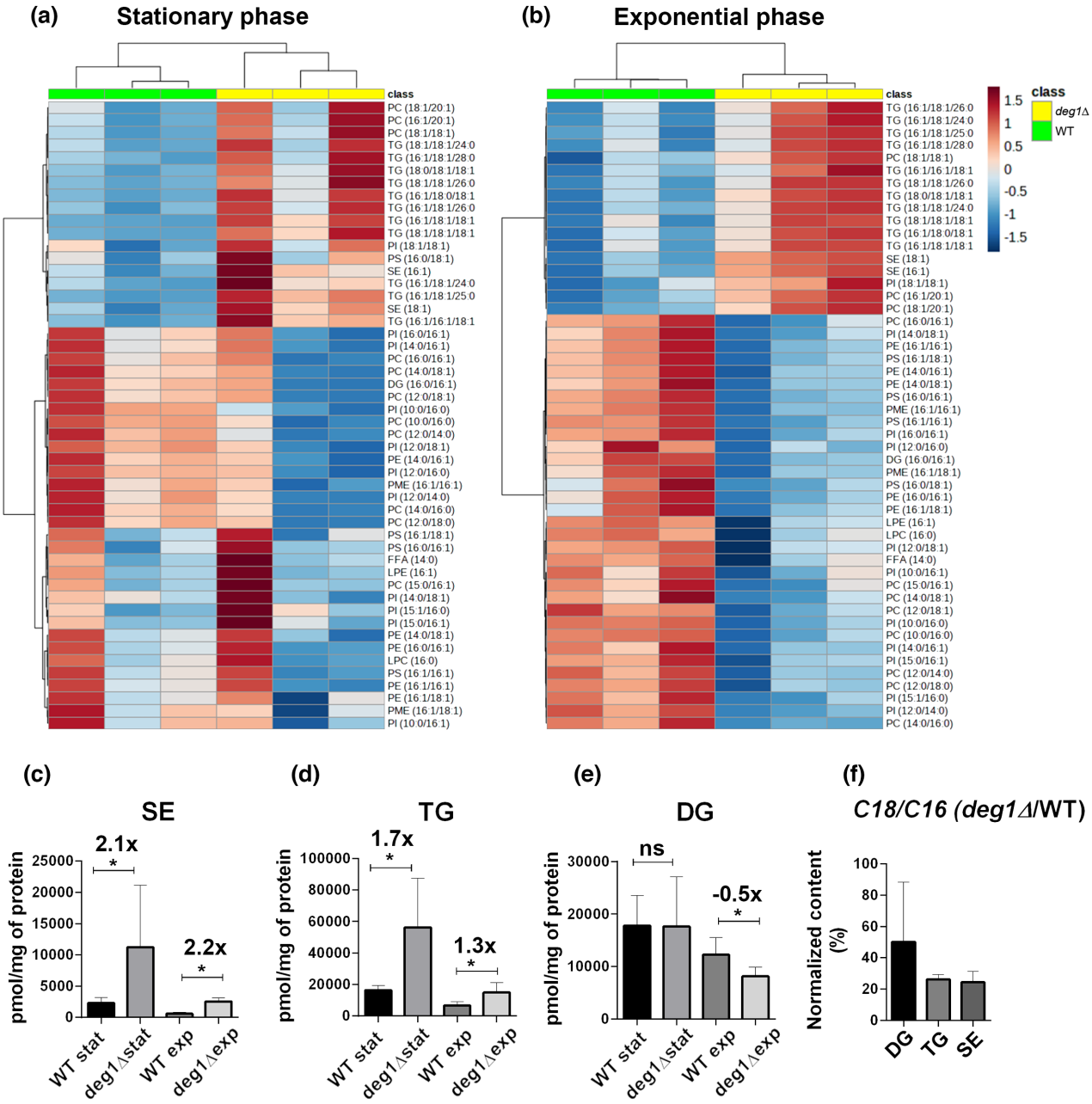

FIGURE 4 Lipidomic profile of WT and *deg1* mutant. (a) Heatmap of distinct clusters of the top 50 significantly changed lipid species in WT and *deg1* mutant grown to stationary phase. The heat map was generated using MetaboAnalyst 5.0, and the significance was determined utilizing ANOVA with adjusted *p*-value (FDR) cutoff: 0.05 and Fisher's post hoc analysis, $n=3$ independent experiments. (b) As in (a) but for WT and *deg1* cells from exponential phase. (c) Levels of steryl ester (SE) from WT and *deg1* cells in stationary (Stat) or exponential (Exp) phase. (d) Levels of triacylglycerol (TG) from WT and *deg1* cells in stationary (Stat) or exponential (Exp) phase. (e) Levels of diacylglycerol (DG) from WT and *deg1* cells in stationary (Stat) or exponential (Exp) phase. Log2 fold changes are indicated above bar diagrams (c–e). The significance was determined utilizing two-tailed *t*-test (*≤0.05; ns-non-significant (f) The ratio of C18/C16 acyl chains of neutral lipids in *deg1* mutant was normalized to WT, both grown to exponential phase. The difference between *deg1* mutant and WT was statistically significant for the neutral lipids shown in the figure ($p \leq 0.05$). (c–f) Data are shown as mean ($n=3$) ± standard deviation of mean (SD).

the top 50 most significantly changed lipid species together with volcano plots (Figure S3a,b) shows that the amount of TG is higher in *deg1* mutant while a lower phospholipid levels are observed in both stationary and exponential phases (Figure 4a,b). Next, we analyzed the total content (sum of all species within a class) of neutral lipids. As shown in Figure 4c,d, neutral lipid synthesis in *S. cerevisiae* is highly regulated and responds to growth phase as a notable increase of total SE and TG occurred at stationary phase in WT cells. Such storage lipid accumulation allows the cells to maintain energy homeostasis in the absence of nutrients. As cells are shifted from starvation condition to a high glucose medium, neutral lipids are mobilized and the resulting fatty acids contribute to formation of phospholipids (Kurat et al., 2006; Rajakumari et al., 2010). These results contrast to those of *deg1* mutant cells where the levels of SE and TG species are significantly higher compared to WT at stationary phase. Although they undergo lipolysis upon shifting to exponential phase, a significantly increased level is maintained in relation to WT (Figure 4c,d). In contrast to TG, diacylglycerol was moderately reduced in the *deg1* mutant at exponential phase and unaffected in stationary phase (Figure 4e). The main TG/SE and FFA species that were deregulated in *deg1* are shown in Figure S4a–e. It should be mentioned that although both SE (18:1) and SE (16:1) were increased (Figure S3a,b), free ergosterol was not significantly altered in *deg1* mutant.

Since SE and TG are upregulated in the *deg1* mutant, we analyzed whether the lipidomic profile of the *deg1* mutant resembled to that reported for the hyperactive *ACC1*^{S1157A} mutant, in which the acyl C18/C16 ratio in cellular lipids and free fatty acids is drastically increased (Hofbauer et al., 2014). Our lipidomic profiles for the *deg1* mutant in contrast revealed that the C18/C16 ratio of free fatty acids and TG/SE acyl chains were not significantly affected in stationary phase. However, a moderate increase of the C18/C16 acyl chain ratio in diacylglycerol, TG and SE was detected exclusively in exponential phase (Figure 4f).

In general, neutral lipid and phospholipid synthesis compete for the limited pool of free fatty acids. Thus, when neutral lipid synthesis is increased, less fatty acids are available for the synthesis of phospholipids, which are readily synthetized when neutral lipids are degraded. Indeed, increased levels of neutral lipid was accompanied by reduced phospholipid content in the *deg1* mutant (Figure 4a,b). Such negative correlation between neutral lipids and phospholipids was also seen in the WT when stationary and exponential growth phases were compared; the content of phospholipids was higher in exponential phase compared to stationary phase, when neutral lipids accumulate (Figure 5a–e). In comparison to the WT at exponential phase, the total content of the phospholipid classes (i.e., phosphatidyl serine, phosphatidyl methylethanolamine, phosphatidylinositol,

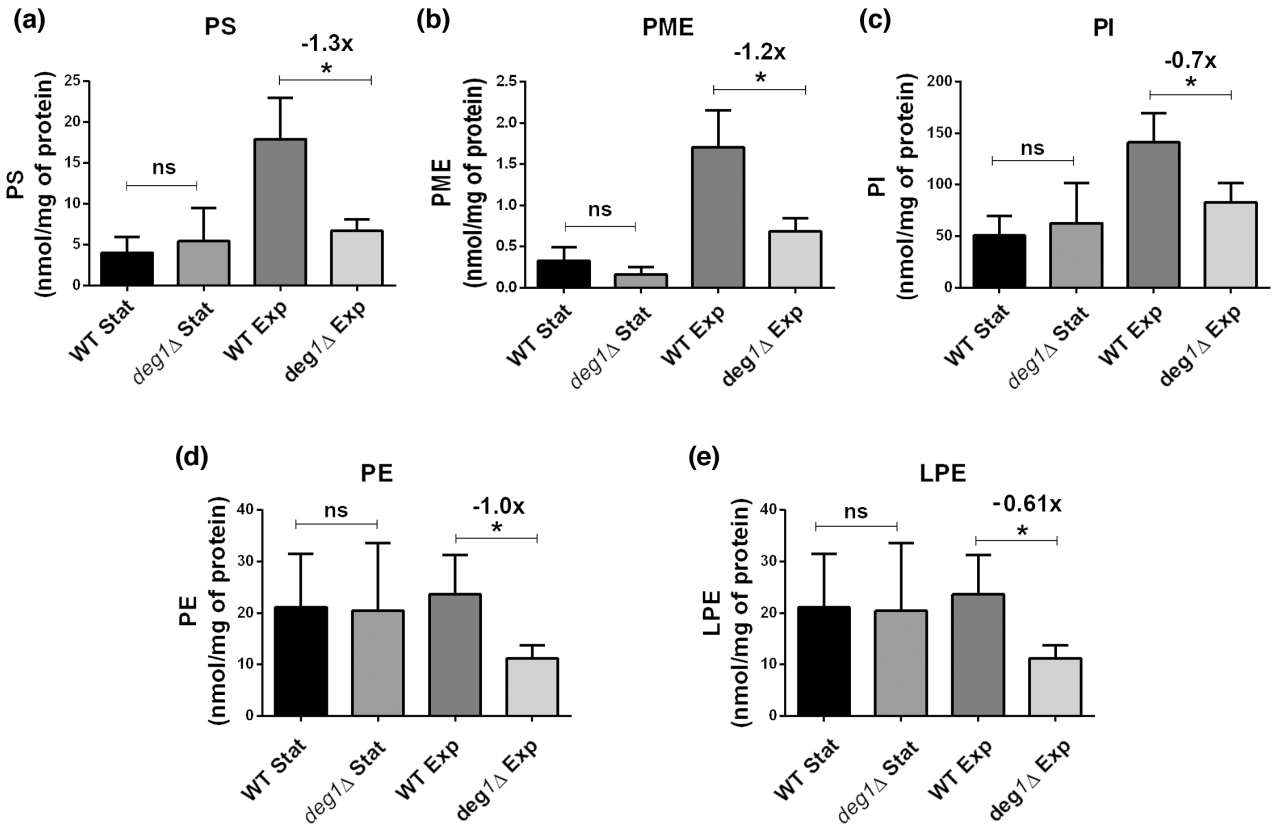

FIGURE 5 The *deg1* mutant shows lower abundance of phospholipid species in relation to WT. Phospholipid species that show a decrease in relative abundance in *deg1* mutant grown to exponential phase: (a) phosphatidylserine (PS), (b) phosphatidyl methylethanolamine (PME), (c) phosphatidylinositol (PI), (d) phosphatidylethanolamine (PE), and (e) lysoPE (LPE). At stationary phase, phospholipid species were not significantly changed in *deg1* mutant compared to WT. Data are shown as mean ($n = 3$) ± standard deviation of mean (SD).

phosphatidylethanolamine, and lysophosphatidylethanolamine), was significantly lower in the *deg1* mutant (Figure 5). Moreover, the *deg1* mutant did not display increased levels of C18 acyl chains in phospholipids as observed in the *ACC1*^{S1157A} mutant (Hofbauer et al., 2014). Our observation of major changes in neutral lipids and phospholipid composition, but not in the general acyl length of all cellular lipids in the tRNA modification mutant, suggests a mechanism distinct from Acc1 activation. Our results indicate that in *deg1* mutant, storage lipids are not degraded properly upon switching to exponential phase, which may limit the availability of precursors for phospholipid synthesis and eventually, result in an imbalance between neutral and phospholipid levels.

3 | DISCUSSION

The tRNA modifier Deg1 is conserved from yeast to humans and mutation of the human *DEG1* orthologue *PUS3* induces neurodegenerative defects partly resembling those described in patients with defects in the tRNA modification complex Elongator (Abdelrahman et al., 2018; Gaik, Kojic, Stegeman, et al., 2022; Gaik, Kojic, Wainwright, et al., 2022; Lin et al., 2022; Shaheen et al., 2016). In yeast, pleiotropic phenotypes of Elongator and *deg1* mutants also overlap, including the induction of protein aggregates and high LD content (Bozaquel-Morais et al., 2018; Khonsari et al., 2021; Nedialkova & Leidel, 2015). Since different types of translational errors are induced in absence of functional Elongator (Joshi et al., 2018; Tavares et al., 2021; Tükenmez et al., 2015), we tested whether loss of Deg1 could also affect translational fidelity. While a tRNA lacking modifications could itself become error-prone in decoding, an indirect effect linked to an inefficiency of correct decoding is also possible (Khonsari & Klassen, 2020; Tavares et al., 2021). We show that in *deg1* mutants two Asn codons read by a Deg1 target tRNA become more efficiently misread by another tRNA not modified by Deg1 (tRNA^{Lys}; Figure S2c). Considering that ribosomal profiling data indicated a larger number of inefficiently decoded codons, such indirect loss of translational fidelity might be more widespread in *deg1* and possibly mechanistically linked to the observed induction of protein aggregates. A similar concept was proposed for protein aggregates induced in Elongator mutants and supported by proteomic analysis (Tavares et al., 2021).

In this study, we investigated the lipid-specific effects of the *deg1* mutation in yeast in more detail. S1157A exchange in Acc1 prevents inhibitory S1157 phosphorylation by Snf1 and in turn upregulates its activity, LD levels and sorA resistance (Hofbauer et al., 2014). Since *ACC1*^{S1157A} and *deg1* mutation induce similar lipid phenotypes, we investigated whether loss of the tRNA modifier could interfere with Acc1 phosphorylation at S1157. Genetic analysis, however, revealed that all analyzed *deg1* lipid phenotypes are independent of S1157 phosphorylation (Figure 1). In addition, *deg1* mutants do not phenocopy *ACC1*^{S1157A} with respect to inositol auxotrophy and the effects of both mutations on specific lipid classes are strikingly distinct.

ACC1^{S1157A} and *snf1* mutants upregulate TG (but not SE) with a concomitant increase of the C18/C16 ratio of acyl chains in fatty acids, TG and phospholipids (Hofbauer et al., 2014). Absence of *DEG1* in contrast strongly induces SE levels, whereas TG levels increase more subtly (Figures 3a–c and 4c,d). In addition, a general increase in the C18/C16 ratio of fatty acyl chains is not observed in *deg1* cells (Figure 4f). These differences support the conclusion that the lipid phenotypes of *deg1* arise independently of changes in Acc1 phosphorylation and activation.

A major effect in *deg1* mutants is the diminished induction of phospholipid synthesis when stationary phase cells are refed with fresh medium and switch to exponential growth. Induction of phospholipid synthesis at the expense of storage lipid depletion is observed in the WT but occurs less efficiently in *deg1* cells (Figure 4). Hence, lipid remodeling to support phospholipid induction is impaired in *deg1*, which might involve reduced activity of lipases involved in storage lipid remobilization. However, published *deg1* transcriptome data (Chou et al., 2017) do not indicate reduced expression of the lipase genes *TGL1*, *TGL3*, *TGL4*, *TGL5* or *YEH1* and *YEH2*. Instead, there are signs of inappropriate stationary phase gene expression programs executed in the absence of nutrient depletion. Similar to Elongator mutants, amino acid biosynthesis genes are globally upregulated in *deg1* and stationary phase marker genes *SNZ1* and *SNO1* (Padilla et al., 1998) are the most strongly induced mRNAs (Chou et al., 2017). This may indicate an altered metabolic state of *deg1* mutants, resembling stationary phase or nutrient depletion. Under such conditions, storage lipid levels are normally high, and lipolysis is inhibited, and these characteristics are observed in the *deg1* mutant despite the refed growth condition and abundant nutrient supply. Hence, the lipid phenotype of *deg1* fits into the assumption of an inappropriate stationary phase metabolic state. Since combined *deg1 elp3* mutants display signs of reduced TOR activity including autophagy activation and gene expression changes (Bruch et al., 2020), it is possible that nutrient availability is incorrectly sensed or signaled in the absence of critical modifications at or around the tRNA anticodon loop. A study in fission yeast further supports the implication of Elongator-dependent tRNA modifications in TOR signaling (Candiracci et al., 2019).

Interestingly, budding yeast TOR is also known to regulate neutral lipid dynamics in yeast (Madeira et al., 2015), and the reduced TOR activity in combined *elp3 deg1* mutants (Bruch et al., 2020) might point to a connection between tRNA modification, TOR activity and lipid homeostasis. In detail, however, TOR inhibition by rapamycin increases TG rather than SE levels (Madeira et al., 2015). Since *deg1* mutation affects SE levels more drastically than TG (Figures 3 and 4), other factors than TOR inhibition alone are likely involved in deregulation of lipid homeostasis in tRNA modification mutants.

It should be noted that U34 tRNA modification defects induce metabolic shifts partly resembling starvation situations (Gupta et al., 2019; Gupta & Laxman, 2020; Karlsborn et al., 2016; Laxman et al., 2013). Also, *deg1* and Elongator mutations were found to significantly alter cellular amino acid levels (Mülleder et al., 2016), demonstrating that distinct tRNA modification defects may similarly

affect metabolism. Such common effect might also be relevant for imbalances in lipid homeostasis observed in this study. In support, a deletion of *TUM1*, a gene required along with Elongator for mcm^5s^2U modification, was found to upregulate SE, but not TG levels, thus resembling part of the *deg1* lipid phenotype (Uršič et al., 2017). In addition, mutations in yeast tRNA genes promoting mistranslation at alanine and glycine codons induce major changes in lipidome composition (Araújo et al., 2018). Hence, common lipid phenotypes may be induced by different tRNA defects and this might represent an additional aspect of the widespread metabolic changes caused by interference with the fine-tuning of tRNA function. It might be speculated that such common effects also contribute to related disease phenotypes in humans carrying mutations in anticodon loop modification genes. Since several of the metabolically important tRNA modifications are also required to maintain proteostasis, it seems possible that lipidomic effects (as observed in *deg1*) are indirect outcomes of protein aggregation which induces mis-activation of nutrient stress responses.

4 | EXPERIMENTAL PROCEDURES

4.1 | Yeast strains

All strains used in this study are listed in Table 1. Standard methods were used for the cultivation of yeast (Sherman, 2002). Yeast strains were grown in yeast peptone dextrose medium (YPD) or in yeast nitrogen base (YNB) minimal medium lacking specific nutrients for selection of mutants and plasmids. Individual gene knockouts were introduced using PCR-based deletion cassettes and the pUG plasmid system as outlined (Gueldener et al., 2002). Yeast transformation was done according to (Gietz & Schiestl, 2007).

Genomic gene editing at the *ACC1* locus was carried out using the CRISPR-Cas vector system described (Laughery et al., 2015). For this purpose, a single guide-RNA expression plasmid was created by ligating hybridized DNA oligos (5′-GATCATCTAAAATGGGTATG AACAGTTTTAGAGCTAG-3′) and (5′-CTAGCTCTAAAACTGTTCAT ACCCATTTTAGAT-3′) into SwaI/BclI digested plasmid pML104 (Laughery et al., 2015). The resulting vector was co-transformed with a dsDNA fragment containing a part of the *ACC1* sequence and the desired S1157A mutation (5′-AGCTGCGTTCTCCACCTTTCCA ACTGTTAAATCTAAAATGGGTATGAACAGAGCTGTTGCTGTTTC AGATTTGTCATATGTTGCAAACAG-3′). The fragment was obtained by hybridization of two complementary oligonucleotides. Colonies were checked for the $ACC1^{S1157A}$ mutation by PCR amplification and sequencing and phenotypically (sorA resistance). Plate assays for yeast phenotyping were conducted as described previously (Bozaquel-Morais et al., 2018).

4.2 | Western blot

To isolate proteins from yeast, liquid cultures were grown in 50 mL YPD overnight at 30°C. The following day, fresh medium was added to adjust cultures to OD600 nm = 0.02 and grown to an OD600 nm = 1.0. Yeast (3 OD units) was harvested, washed and resuspended in 0.1 M NaOH followed by incubation for 10 min (Kushnirov et al., 2006). Cells were washed, resuspended in 50 μL 5× Laemmli buffer (312.5 mM Tris–HCl pH 6.8, 10% SDS w/v, 50% glycerol v/v, 25% β-mercaptoethanol v/v, 0.01% bromophenol blue w/v) and incubated for 10 min at 99°C. After separation of proteins by SDS-PAGE, transfer to PVDF membranes was carried out using the Mini PROTEAN® system (Bio-Rad) following recommendations by the supplier. Detection of Acc1-GFP and Cdc19 involved specific

TABLE 1 Strains used in this study.

Strain	Genotype	Source
BY4741	*MATa; his3Δ, leu2Δ, met15Δ, ura3Δ*	Euroscarf
deg1	BY4741 *deg1Δ::kanMX4*	Euroscarf
snf1	BY4741 *snf1Δ::kanMX4*	Euroscarf
ino1	BY4741 *ino1Δ::kanMX4*	Euroscarf
opi1	BY4741 *opi1Δ::kanMX4*	Euroscarf
reg1	BY4741 *reg1Δ::kanMX4*	Euroscarf
reg1 deg1	BY4741 *reg1Δ::kanMX4; deg1Δ::SpHIS3*	This study
$ACC1^{S1157A}$	BY4741 *ACC1S1157A*	This study
deg1 $ACC1^{S1157A}$	BY4741 *deg1Δ::kanMX4;* $ACC1^{S1157A}$	This study
ACC1-GFP	BY4741 *ACC1-GFP::HIS3MX*	Huh et al. (2003)
deg1 ACC1-GFP	BY4741 *ACC1-GFP::HIS3MX; deg1Δ::KILEU2*	This study
snf1 ACC1-GFP	BY4741 *ACC1-GFP::HIS3MX; snf1Δ::KIURA3*	This study
snf1 deg1 ACC1-GFP	BY4741 *ACC1-GFP::HIS3MX; snf1Δ::KIURA3; deg1Δ::KILEU2*	This study
$ACC1^{S1157A}$*-GFP*	BY4741 *ACC1-GFP::HIS3MX;* $ACC1^{S1157A}$	This study
deg1 met22	BY4741 *deg1Δ::SpHIS5 met22Δ::KILEU2*	Khonsari and Klassen (2020)

antibodies obtained from Santa Cruz Biotechnology (USA) and Thorner lab (University of California, USA).

4.3 | Codon-specific misreading

Misreading assay was conducted using renilla/firefly luciferase plasmids pDB688 (normalization control), pDB825, pDB827, pDB872 and pDB865 (Salas-Marco & Bedwell, 2005). Plasmids were transformed into wild type and *deg1* mutants and individual colonies used to inoculate uracil-free YNB medium. Renilla and firefly luminescence from independent cultures was measured using the dual luciferase reporter assay kit (Promega, Fitchburg, USA) and a GloMax luminometer (Promega). Ten biological replicates were conducted for each strain and condition and three technical replicates were measured per culture. Mistranslation rates were calculated as described before (Khonsari & Klassen, 2020).

4.4 | LD analysis by BODIPY staining

To visualize LDs, the fluorescent dye BODIPY® 493/503 was used. A 5 mM stock solution was prepared in 100% DMSO and stored at −20°C until used. To stain cells, 1–5 μL of BODIPY® 493/503 stock solution was added to formaldehyde-fixed cells and mixed carefully. The suspension was incubated in the dark for 10 min and washed. Cells were examined using an Olympus BX53 microscope (GFP channel with 200 ms exposure). Pictures were taken with the CellSens Standard software (Olympus), and fluorescent intensity was analyzed with Fiji (Schindelin et al., 2012).

4.5 | Neutral lipid analysis by thin layer chromatography

Lipids were extracted from yeast cells based on a Bligh and Dyer modified protocol (Bourque & Titorenko, 2009), dried under nitrogen and stored −20°C until used. Neutral lipids were separated in silica plates using a two-step separation system. The first separation to 2/3 of the height of the plate used light petroleum/diethyl ether/acetic acid (35:15:1 v/v) as a solvent system, followed by light petroleum/diethyl ether (49:1 v/v) solvent (Schmidt et al., 2013). The standards used were SE, TG, diacylglycerol, free fatty acids and monoacylglycerol (Sigma-Aldrich St. Louis, MO). Lipids were revealed with iodine vapor and quantified by densitometry using Image Master TotalLab 1.11 (Amersham Pharmacia Biotech, UK).

4.6 | Lipidomic assay

Yeast cells were inoculated in fresh YPD at a low density (OD 600 nm = 0.3) and collected after 7 or 48 h. Cells were lyophilized and sent frozen to the lipidomics facility at the Biochemistry Institute, São Paulo University, São Paulo, Brazil. Approximately 200 mg of lyophilized cells was resuspended in 350 μL of deionized water. Cells were disrupted by glass beads in cold environment. Lipid extraction was conducted using the m ethyl-tert-butyl ether (MTBE) method as previously described (Matyash et al., 2008) with modifications. Yeast lysate samples (100 μL) were mixed with 100 μL of an internal standard mix (Table S1) and 300 μL methanol containing butylated hydroxytoluene (BHT, 10 μM) as antioxidant. Samples were vortexed for 30 s and then incubated with MTBE (1 mL) in a Thermomixer (1000 rpm at 20°C) for 1 h. Phase separation was induced by adding water (300 μL), vortexing for 30 s and centrifugation at 1000 *g* for 10 min. The upper organic phase was collected, dried with nitrogen gas and dissolved in 100 μL isopropanol. The analysis of extracts containing internal standards of different classes of lipids was performed by high-performance liquid chromatography (UPLC Nexera, Shimadzu, Kyoto, Japan) coupled with ESI-TOF/MS mass spectrometry (Triple TOF 6600, Sciex, Concord, USA; Chaves-Filho et al., 2019).

The sample injection volume was adjusted to 2 μL, and the compounds were separated on a CORTECS® column (C18, 1.6 μm, 2.1 × 100 mm) with a flow rate of 0.2 mL/min and oven temperature at 35°C. The mobile phase was composed of (A) water/acetonitrile (60:40) and (B) isopropanol/acetonitrile/water (88:10:2). A and B contain ammonium acetate or ammonium formate at a final concentration of 10 mM for experiments performed in negative or positive ionization mode, respectively. The following gradient was used in the chromatography: from 40% to 100% B over the first 10 min; 100% B from 10 to 12 min; and 100% to 40% B for 12–13 min, holding 40% B for 13–20 min. Mass spectrometry was operated in both ionization modes (positive and negative), with the "scan" performed for mass values of 200–2000 Da. MS/MS data acquisition was performed using the Analyst® 1.7.1 software; proceeding to their analysis with the PeakView® software. The lipid molecular species were identified and then quantified using the MultiQuant® software. The precursor ions areas were normalized by the internal standards. The MetaboAnalyst (http://www.metaboanalyst.ca) was used for statistical analyses of the lipidomic data. Univariate statistical tests included analysis of variance (one-way ANOVA) or volcano plot (*t*-test and fold-change). Data from univariate analyses were also plotted as heatmaps taking into account the lowest *p*-values. The complete set of results is found in Table S2.

AUTHOR CONTRIBUTIONS

Roland Klassen: Writing – original draft; writing – review and editing; funding acquisition; data curation; validation; conceptualization. **Gabriel Soares Matos:** Investigation; data curation; writing – review and editing. **Leonie Vogt:** Investigation; data curation; writing – review and editing. **Rosangela Silva Santos:** Investigation; writing – review and editing; data curation. **Aurélien Devillars:** Investigation; data curation. **Marcos Yukio Yoshinaga:** Methodology; writing – review and editing; data curation; validation. **Sayuri Miyamoto:** Writing – review and editing;

data curation. **Raffael Schaffrath:** Writing – review and editing; funding acquisition; data curation; validation; conceptualization. **Monica Montero-Lomeli:** Writing – original draft; writing – review and editing; funding acquisition; data curation; validation; conceptualization.

ACKNOWLEDGEMENTS

We thank D. Bedwell for providing plasmids. A cooperation initiation grant between Deutsche Forschungsgemeinschaft (DFG) to R.S. (SCHA750/19); SCHA750/18 and Fundação Carlos Chagas Filho de Amparo à Pesquisa do Estado do Rio de Janeiro (FAPERJ) to M.M.L. is greatly acknowledged. Funding by the DFG Priority Program SPP1784 "Chemical Biology of Native Nucleic Acid Modifications" to R.S. (SCHA750/20), R.K. (KL2937/1) and by FAPERJ E26/210446/2019 and E26/201.070/2021 to M.M.L. is gratefully acknowledged. G.S.M. was supported by Conselho Nacional de Desenvolvimento Científico e Tecnológico (CNPq), and S.M. was supported by Fundação de Amparo à Pesquisa do Estado de São Paulo (FAPESP, CEPID–Redoxoma 13/07937-8) and CNPq 313926/2021-2. Open access funding by project DEAL is greatly acknowledged. Open Access funding enabled and organized by Projekt DEAL.

DATA AVAILABILITY STATEMENT

The data that support the findings of this study are available in the supplementary material of this article.

ETHICS STATEMENT

The authors declare that no human or animal subjects were used in this study.

ORCID

Raffael Schaffrath https://orcid.org/0000-0001-9484-5247
Roland Klassen https://orcid.org/0000-0002-0809-0050

REFERENCES

Abdelrahman, H.A., Al-Shamsi, A.M., Ali, B.R. & Al-Gazali, L. (2018) A null variant in PUS3 confirms its involvement in intellectual disability and further delineates the associated neurodevelopmental disease. *Clinical Genetics*, 94, 586–587. Available from: https://doi.org/10.1111/cge.13443

Araújo, A.R.D., Melo, T., Maciel, E.A., Pereira, C., Morais, C.M., Santinha, D.R. et al. (2018) Errors in protein synthesis increase the level of saturated fatty acids and affect the overall lipid profiles of yeast. *PLoS One*, 13, e0202402. Available from: https://doi.org/10.1371/journal.pone.0202402

Barraud, P., Gato, A., Heiss, M., Catala, M., Kellner, S. & Tisné, C. (2019) Time-resolved NMR monitoring of tRNA maturation. *Nature Communications*, 10, 3373. Available from: https://doi.org/10.1038/s41467-019-11356-w

Boccaletto, P., Machnicka, M.A., Purta, E., Piatkowski, P., Baginski, B., Wirecki, T.K. et al. (2018) MODOMICS: a database of RNA modification pathways. 2017 update. *Nucleic Acids Research*, 46, D303–D307. Available from: https://doi.org/10.1093/nar/gkx1030

Bourque, S.D. & Titorenko, V.I. (2009) A quantitative assessment of the yeast lipidome using electrospray ionization mass spectrometry. *Journal of Visualized Experiments*, 30, 1513. Available from: https://doi.org/10.3791/1513

Bozaquel-Morais, B.L., Madeira, J.B., Maya-Monteiro, C.M., Masuda, C.A. & Montero-Lomeli, M. (2010) A new fluorescence-based method identifies protein phosphatases regulating lipid droplet metabolism. *PLoS One*, 5, e13692. Available from: https://doi.org/10.1371/journal.pone.0013692

Bozaquel-Morais, B.L., Madeira, J.B., Venâncio, T.M., Pacheco-Rosa, T., Masuda, C.A. & Montero-Lomeli, M. (2017) A chemogenomic screen reveals novel Snf1p/AMPK independent regulators of acetyl-CoA carboxylase. *PLoS One*, 12, e0169682. Available from: https://doi.org/10.1371/journal.pone.0169682

Bozaquel-Morais, B.L., Vogt, L., D'Angelo, V., Schaffrath, R., Klassen, R. & Montero-Lomelí, M. (2018) Protein phosphatase Sit4 affects lipid droplet synthesis and Soraphen A resistance independent of its role in regulating elongator dependent tRNA modification. *Biomolecules*, 8. Available from: https://doi.org/10.3390/biom8030049

Bruch, A., Laguna, T., Butter, F., Schaffrath, R. & Klassen, R. (2020) Misactivation of multiple starvation responses in yeast by loss of tRNA modifications. *Nucleic Acids Research*, 48, 7307–7320. Available from: https://doi.org/10.1093/nar/gkaa455

Candiracci, J., Migeot, V., Chionh, Y.-H., Bauer, F., Brochier, T., Russell, B. et al. (2019) Reciprocal regulation of TORC signaling and tRNA modifications by elongator enforces nutrient-dependent cell fate. *Science Advances*, 5, eaav0184. Available from: https://doi.org/10.1126/sciadv.aav0184

Chaves-Filho, A.B., Pinto, I.F.D., Dantas, L.S., Xavier, A.M., Inague, A., Faria, R.L. et al. (2019) Alterations in lipid metabolism of spinal cord linked to amyotrophic lateral sclerosis. *Scientific Reports*, 9, 11642. Available from: https://doi.org/10.1038/s41598-019-48059-7

Chou, H.-J., Donnard, E., Gustafsson, H.T., Garber, M. & Rando, O.J. (2017) Transcriptome-wide analysis of roles for tRNA modifications in translational regulation. *Molecular Cell*, 68, 978–992.e4. Available from: https://doi.org/10.1016/j.molcel.2017.11.002

Donahue, T.F. & Henry, S.A. (1981) myo-Inositol-1-phosphate synthase. Characteristics of the enzyme and identification of its structural gene in yeast. *The Journal of Biological Chemistry*, 256, 7077–7085.

Gaik, M., Kojic, M., Stegeman, M.R., Öncü-Öner, T., Kościelniak, A., Jones, A. et al. (2022) Functional divergence of the two elongator subcomplexes during neurodevelopment. *EMBO Molecular Medicine*, 14, e15608. Available from: https://doi.org/10.15252/emmm.202115608

Gaik, M., Kojic, M., Wainwright, B.J. & Glatt, S. (2022) Elongator and the role of its subcomplexes in human diseases. *EMBO Mol Med*, 15, e16418. Available from: https://doi.org/10.15252/emmm.202216418

Gietz, R.D. & Schiestl, R.H. (2007) High-efficiency yeast transformation using the LiAc/SS carrier DNA/PEG method. *Nature Protocols*, 2, 31–34. Available from: https://doi.org/10.1038/nprot.2007.13

Greenberg, M.L., Reiner, B. & Henry, S.A. (1982) Regulatory mutations of inositol biosynthesis in yeast: isolation of inositol-excreting mutants. *Genetics*, 100, 19–33. Available from: https://doi.org/10.1093/genetics/100.1.19

Gueldener, U., Heinisch, J., Koehler, G.J., Voss, D. & Hegemann, J.H. (2002) A second set of loxP marker cassettes for cre-mediated multiple gene knockouts in budding yeast. *Nucleic Acids Research*, 30, e23.

Gupta, R. & Laxman, S. (2020) tRNA wobble-uridine modifications as amino acid sensors and regulators of cellular metabolic state. *Current Genetics*, 66, 475–480. Available from: https://doi.org/10.1007/s00294-019-01045-y

Gupta, R., Walvekar, A.S., Liang, S., Rashida, Z., Shah, P. & Laxman, S. (2019) A tRNA modification balances carbon and nitrogen metabolism by regulating phosphate homeostasis. *eLife*, 8. Available from: https://doi.org/10.7554/eLife.44795

Han, L., Guy, M.P., Kon, Y. & Phizicky, E.M. (2018) Lack of 2'-O-methylation in the tRNA anticodon loop of two phylogenetically distant yeast species activates the general amino acid control pathway. *PLoS Genetics*, 14, e1007288. Available from: https://doi.org/10.1371/journal.pgen.1007288

Han, L., Kon, Y. & Phizicky, E.M. (2015) Functional importance of Ψ38 and Ψ39 in distinct tRNAs, amplified for tRNAGln(UUG) by unexpected temperature sensitivity of the s2U modification in yeast. *RNA*, 21, 188–201. Available from: https://doi.org/10.1261/rna.048173.114

Hofbauer, H.F., Schopf, F.H., Schleifer, H., Knittelfelder, O.L., Pieber, B., Rechberger, G.N. et al. (2014) Regulation of gene expression through a transcriptional repressor that senses acyl-chain length in membrane phospholipids. *Developmental Cell*, 29, 729–739. Available from: https://doi.org/10.1016/j.devcel.2014.04.025

Huh, W.K., Falvo, J.V., Gerke, L.C., Carroll, A.S., Howson, R.W., Weissman, J.S. et al. (2003) Global analysis of protein localization in budding yeast. *Nature*, 425(6959), 686–691. Available from: https://doi.org/10.1038/nature02026

Joshi, K., Bhatt, M.J. & Farabaugh, P.J. (2018) Codon-specific effects of tRNA anticodon loop modifications on translational misreading errors in the yeast *Saccharomyces cerevisiae*. *Nucleic Acids Research*, 46, 10331–10339. Available from: https://doi.org/10.1093/nar/gky664

Jühling, F., Mörl, M., Hartmann, R.K., Sprinzl, M., Stadler, P.F. & Pütz, J. (2009) tRNAdb 2009: compilation of tRNA sequences and tRNA genes. *Nucleic Acids Research*, 37, D159–D162. Available from: https://doi.org/10.1093/nar/gkn772

Karlsborn, T., Mahmud, A.K.M.F., Tükenmez, H. & Byström, A.S. (2016) Loss of ncm5 and mcm5 wobble uridine side chains results in an altered metabolic profile. *Metabolomics*, 12, 177. Available from: https://doi.org/10.1007/s11306-016-1120-8

Khonsari, B. & Klassen, R. (2020) Impact of Pus1 Pseudouridine synthase on specific decoding events in *Saccharomyces cerevisiae*. *Biomolecules*, 10. Available from: https://doi.org/10.3390/biom10050729

Khonsari, B., Klassen, R. & Schaffrath, R. (2021) Role of SSD1 in phenotypic variation of *Saccharomyces cerevisiae* strains lacking DEG1-dependent Pseudouridylation. *International Journal of Molecular Sciences*, 22. Available from: https://doi.org/10.3390/ijms22168753

Klassen, R., Ciftci, A., Funk, J., Bruch, A., Butter, F. & Schaffrath, R. (2016) tRNA anticodon loop modifications ensure protein homeostasis and cell morphogenesis in yeast. *Nucleic Acids Research*, 44, 10946–10959. Available from: https://doi.org/10.1093/nar/gkw705

Klassen, R. & Schaffrath, R. (2017) Role of Pseudouridine formation by Deg1 for functionality of two glutamine Isoacceptor tRNAs. *Biomolecules*, 7. Available from: https://doi.org/10.3390/biom7010008

Kurat, C.F., Natter, K., Petschnigg, J., Wolinski, H., Scheuringer, K., Scholz, H. et al. (2006) Obese yeast: triglyceride lipolysis is functionally conserved from mammals to yeast. *The Journal of Biological Chemistry*, 281, 491–500. Available from: https://doi.org/10.1074/jbc.M508414200

Kushnirov, V.V., Alexandrov, I.M., Mitkevich, O.V., Shkundina, I.S. & Ter-Avanesyan, M.D. (2006) Purification and analysis of prion and amyloid aggregates. *Methods*, 39, 50–55. Available from: https://doi.org/10.1016/j.ymeth.2006.04.007

Laughery, M.F., Hunter, T., Brown, A., Hoopes, J., Ostbye, T., Shumaker, T. et al. (2015) New vectors for simple and streamlined CRISPR-Cas9 genome editing in *Saccharomyces cerevisiae*. *Yeast*, 32, 711–720. Available from: https://doi.org/10.1002/yea.3098

Laxman, S., Sutter, B.M., Wu, X., Kumar, S., Guo, X., Trudgian, D.C. et al. (2013) Sulfur amino acids regulate translational capacity and metabolic homeostasis through modulation of tRNA thiolation. *Cell*, 154, 416–429. Available from: https://doi.org/10.1016/j.cell.2013.06.043

Lecointe, F., Simos, G., Sauer, A., Hurt, E.C., Motorin, Y. & Grosjean, H. (1998) Characterization of yeast protein Deg1 as pseudouridine synthase (Pus3) catalyzing the formation of psi 38 and psi 39 in tRNA anticodon loop. *The Journal of Biological Chemistry*, 273, 1316–1323.

Lin, T.-Y., Smigiel, R., Kuzniewska, B., Chmielewska, J.J., Kosińska, J., Biela, M. et al. (2022) Destabilization of mutated human PUS3 protein causes intellectual disability. *Human Mutation*, 43, 2063–2078. Available from: https://doi.org/10.1002/humu.24471

Madeira, J.B., Masuda, C.A., Maya-Monteiro, C.M., Matos, G.S., Montero-Lomelí, M. & Bozaquel-Morais, B.L. (2015) TORC1 inhibition induces lipid droplet replenishment in yeast. *Molecular and Cellular Biology*, 35, 737–746. Available from: https://doi.org/10.1128/MCB.01314-14

Matyash, V., Liebisch, G., Kurzchalia, T.V., Shevchenko, A. & Schwudke, D. (2008) Lipid extraction by methyl-tert-butyl ether for high-throughput lipidomics. *Journal of Lipid Research*, 49, 1137–1146. Available from: https://doi.org/10.1194/jlr.D700041-JLR200

Mülleder, M., Calvani, E., Alam, M.T., Wang, R.K., Eckerstorfer, F., Zelezniak, A. et al. (2016) Functional metabolomics describes the yeast biosynthetic regulome. *Cell*, 167, 553–565.e12. Available from: https://doi.org/10.1016/j.cell.2016.09.007

Nedialkova, D.D. & Leidel, S.A. (2015) Optimization of codon translation rates via tRNA modifications maintains proteome integrity. *Cell*, 161, 1606–1618. Available from: https://doi.org/10.1016/j.cell.2015.05.022

Padilla, P.A., Fuge, E.K., Crawford, M.E., Errett, A. & Werner-Washburne, M. (1998) The highly conserved, coregulated SNO and SNZ gene families in *Saccharomyces cerevisiae* respond to nutrient limitation. *Journal of Bacteriology*, 180, 5718–5726. Available from: https://doi.org/10.1128/JB.180.21.5718-5726.1998

Phizicky, E.M. & Hopper, A.K. (2010) tRNA biology charges to the front. *Genes & Development*, 24, 1832–1860. Available from: https://doi.org/10.1101/gad.1956510

Phizicky, E.M. & Hopper, A.K. (2023) The life and times of a tRNA. *RNA*, 29, 898–957. Available from: https://doi.org/10.1261/rna.079620.123

Rajakumari, S., Rajasekharan, R. & Daum, G. (2010) Triacylglycerol lipolysis is linked to sphingolipid and phospholipid metabolism of the yeast *Saccharomyces cerevisiae*. *Biochimica et Biophysica Acta*, 1801, 1314–1322. Available from: https://doi.org/10.1016/j.bbalip.2010.08.004

Ruiz, A., Xu, X. & Carlson, M. (2011) Roles of two protein phosphatases, Reg1-Glc7 and Sit4, and glycogen synthesis in regulation of SNF1 protein kinase. *Proceedings of the National Academy of Sciences of the United States of America*, 108, 6349–6354. Available from: https://doi.org/10.1073/pnas.1102758108

Salas-Marco, J. & Bedwell, D.M. (2005) Discrimination between defects in elongation fidelity and termination efficiency provides mechanistic insights into translational readthrough. *Journal of Molecular Biology*, 348, 801–815. Available from: https://doi.org/10.1016/j.jmb.2005.03.025

Schaffrath, R. & Leidel, S.A. (2017) Wobble uridine modifications–a reason to live, a reason to die?! *RNA Biology*, 14, 1209–1222. Available from: https://doi.org/10.1080/15476286.2017.1295204

Schindelin, J., Arganda-Carreras, I., Frise, E., Kaynig, V., Longair, M., Pietzsch, T. et al. (2012) Fiji: an open-source platform for biological-image analysis. *Nature Methods*, 9, 676–682. Available from: https://doi.org/10.1038/nmeth.2019

Schmidt, C., Ploier, B., Koch, B. & Daum, G. (2013) Analysis of yeast lipid droplet proteome and lipidome. *Methods in Cell Biology*, 116, 15–37. Available from: https://doi.org/10.1016/B978-0-12-408051-5.00002-4

Shaheen, R., Abdel-Salam, G.M.H., Guy, M.P., Alomar, R., Abdel-Hamid, M.S., Afifi, H.H. et al. (2015) Mutation in WDR4 impairs tRNA m(7) G46 methylation and causes a distinct form of microcephalic primordial dwarfism. *Genome Biology*, 16, 210. Available from: https://doi.org/10.1186/s13059-015-0779-x

Shaheen, R., Han, L., Faqeih, E., Ewida, N., Alobeid, E., Phizicky, E.M. et al. (2016) A homozygous truncating mutation in PUS3 expands the role of tRNA modification in normal cognition. *Human Genetics*, 135, 707–713. Available from: https://doi.org/10.1007/s00439-016-1665-7

Shen, Y., Volrath, S.L., Weatherly, S.C., Elich, T.D. & Tong, L. (2004) A mechanism for the potent inhibition of eukaryotic acetyl-coenzyme A carboxylase by soraphen A, a macrocyclic polyketide natural product. *Molecular Cell*, 16, 881–891. Available from: https://doi.org/10.1016/j.molcel.2004.11.034

Sherman, F. (2002) Getting started with yeast. *Methods in Enzymology*, 350, 3–41.

Shi, S., Chen, Y., Siewers, V. & Nielsen, J. (2014) Improving production of malonyl coenzyme A-derived metabolites by abolishing Snf1-dependent regulation of Acc1. *mBio*, 5, e01130-14. Available from: https://doi.org/10.1128/mBio.01130-14

Shin, G.-H., Veen, M., Stahl, U. & Lang, C. (2012) Overexpression of genes of the fatty acid biosynthetic pathway leads to accumulation of sterols in *Saccharomyces cerevisiae*. *Yeast*, 29, 371–383. Available from: https://doi.org/10.1002/yea.2916

Shirra, M.K., Patton-Vogt, J., Ulrich, A., Liuta-Tehlivets, O., Kohlwein, S.D., Henry, S.A. et al. (2001) Inhibition of acetyl coenzyme A carboxylase activity restores expression of the INO1 gene in a snf1 mutant strain of *Saccharomyces cerevisiae*. *Molecular and Cellular Biology*, 21, 5710–5722. Available from: https://doi.org/10.1128/MCB.21.17.5710-5722.2001

Tavares, J.F., Davis, N.K., Poim, A., Reis, A., Kellner, S., Sousa, I. et al. (2021) tRNA-modifying enzyme mutations induce codon-specific mistranslation and protein aggregation in yeast. *RNA Biology*, 18, 563–575. Available from: https://doi.org/10.1080/15476286.2020.1819671

Tükenmez, H., Xu, H., Esberg, A. & Byström, A.S. (2015) The role of wobble uridine modifications in +1 translational frameshifting in eukaryotes. *Nucleic Acids Research*, 43, 9489–9499. Available from: https://doi.org/10.1093/nar/gkv832

Uršič, K., Ogrizović, M., Kordiš, D., Natter, K. & Petrovič, U. (2017) Tum1 is involved in the metabolism of sterol esters in *Saccharomyces cerevisiae*. *BMC Microbiology*, 17, 181. Available from: https://doi.org/10.1186/s12866-017-1088-1

Vahlensieck, H.F., Pridzun, L., Reichenbach, H. & Hinnen, A. (1994) Identification of the yeast ACC1 gene product (acetyl-CoA carboxylase) as the target of the polyketide fungicide soraphen A. *Current Genetics*, 25, 95–100. Available from: https://doi.org/10.1007/BF00309532

SUPPORTING INFORMATION

Additional supporting information can be found online in the Supporting Information section at the end of this article.

How to cite this article: Matos, G.S., Vogt, L., Santos, R.S., Devillars, A., Yoshinaga, M.Y., Miyamoto, S. et al. (2023) Lipidome remodeling in response to nutrient replenishment requires the tRNA modifier Deg1/Pus3 in yeast. *Molecular Microbiology*, 120, 893–905. Available from: https://doi.org/10.1111/mmi.15185